Numerical Simulation of Complex Inhomogeneous Bodies of Revolution

Y. B. Zhai[1], J. F. Zhang[2], T. J. Cui[3]
1. No. 38 Research Institute, Cetc, Hefei 230031, China;
2, 3. Department of Radio Engineering, Southeast University, Nanjing 210096, China

***Abstract*-A hybrid technique is presented that combines the finite element and boundary integral methods for simulating electromagnetic scattering from complex inhomogeneous bodies of revolution. In the proposed method, higher order elements are used in the interior FEM region, first-order elements are used in the surface MOM region. The method has been successfully applied to investigate scattering by penetrable axisymmetric devices with inhomogeneous and anisotropic permittivity and permeability, which is important and helpful to analyze the scattering characteristics of metamaterials.**

I. INTRODUCTION

Electromagnetic scattering from bodies of revolution (BOR) has been studied extensively. The rotational symmetry of the scatterer allows the problem to be solved efficiently using a two-dimensional (2D) computational technique.

A very popular method is the method of moments (MoM) based on integral equation formulations. For homogeneous scatterers [1]-[7], such as perfect conductors, homogeneous dielectrics, integral formulation only requires a surface discretization and automatically take into account the radiation condition. Moreover, the generation of the elements of the method of moments' matrix occupies a major portion of the computational time and many method is presented for accurately and efficiently evaluating the oscillating integrals [2]-[3]. However, MoM formulations yield a dense full matrix, and computational complexity becomes very large for inhomogeneous general materials that require volume MoM [4].

The finite-element method (FEM), which yields a sparse banded matrix, is characterized by very flexible material handling capabilities and is often preferred over the MoM for problems involving complex structures and inhomogeneous materials. When applied to the open-region problems, the FEM mesh must be truncated by an artificial boundary to obtain a bounded computational domain, and to render the problem manageable. Perfectly Matched Layers (PML) is one useful way for mesh truncation without altering the sparsity of the FEM matrix [5]. In order reduce the significant artificial reflection of PMLs at near grazing angles, PML need to be placed at a distance away from the BOR surface. Another widely used method is the hybrid finite element method, which uses a boundary integral to truncate the FEM mesh [6]-[7]. The method has the advantages of both the integral equation methods and the FEM. The integral equation mesh used to truncate the interior finite element region can be made very close to the body, while the FEM mesh is capable of modeling complex inhomogeneous materials.

In this paper, we present a hybrid technique that combines the finite element and boundary integral methods for simulating electromagnetic scattering from complex inhomogeneous bodies of revolution. In the proposed method, higher order elements are used in the interior FEM region, first-order elements are used in the surface MOM region. The method has been successfully applied to investigate scattering by penetrable axisymmetric devices with inhomogeneous and anisotropic permittivity and permeability, which is important and helpful to analyze the scattering characteristics of metamaterials.

II. FORMULATIONS

The object and surrounding space are broken into interior regions and the freespace regions out to a defined surface. In the interior region, a finite-element discretization of a weak form of the wave equation is used to model the geometry and the electric fields [8]:

$$\iiint_V \left[(\nabla \times \boldsymbol{E}^*) \cdot \bar{\bar{\mu}}_r^{-1} \cdot (\nabla \times \boldsymbol{E}) - k_0^2 \boldsymbol{E}^* \cdot \bar{\bar{\varepsilon}}_r^{-1} \cdot \boldsymbol{E} \right] - jk_0 \eta \iint_s \boldsymbol{E}^* \cdot (\hat{n} \times \boldsymbol{E}) dS = 0 \tag{1}$$

in which k_0 is the free space wave number, η_0 is the intrinsic impedance of free space, $\bar{\bar{\mu}}_r$ and $\bar{\bar{\varepsilon}}_r$ are the relative permittivity and permeability of the medium, which have the following symmetry form:

$$\bar{\bar{\mu}}_r = \begin{pmatrix} \mu_{\rho\rho} & 0 & \mu_{\rho z} \\ 0 & \mu_{\phi\phi} & 0 \\ \mu_{\rho z} & 0 & \mu_{zz} \end{pmatrix}, \quad \bar{\bar{\varepsilon}}_r = \begin{pmatrix} \varepsilon_{\rho\rho} & 0 & \varepsilon_{\rho z} \\ 0 & \varepsilon_{\phi\phi} & 0 \\ \varepsilon_{\rho z} & 0 & \varepsilon_{zz} \end{pmatrix}. \tag{2}$$

S is the surface of the penetrable object V, and $\hat{n}$ in the normal vector on S, pointing from object into the free space region. $\boldsymbol{E}^*$ is an appropriately chosen set of testing functions, which is known. The entire electric field $\boldsymbol{E}$ inside the body and $\hat{n} \times \boldsymbol{H}$ on the boundary are the unknown quantities to be determined.

On the boundary S, Fictitious electric $\boldsymbol{J} = \hat{n} \times \boldsymbol{H}$ and magnetic $\boldsymbol{M} = -\hat{n} \times \boldsymbol{E}$ surface currents, equivalent to the tangential magnetic and electric fields just on the exterior of the boundary surface, are defined. These currents produce the true field outside V and zero field inside V. $\boldsymbol{J} = \hat{n} \times \boldsymbol{H}$ could be substituted directly into (1) thereby enforcing continuity of the tangential magnetic field between interior and exterior regions. Following the hybridization procedure of FEM and

MoM described in [6], the other two formulations for the relationship between $\boldsymbol{E}$, $\boldsymbol{J}$ and $\boldsymbol{M}$ are:

$$\iint_S [\boldsymbol{J}^* \cdot \boldsymbol{E} - \boldsymbol{J}^* \cdot K(\boldsymbol{M}) - \boldsymbol{J}^* \cdot \frac{1}{2}\hat{n} \times \boldsymbol{M} + \boldsymbol{J}^* \cdot L(\boldsymbol{J})]dS = \iint_S \boldsymbol{J}^* \cdot \boldsymbol{E}^i dS \tag{3}$$

$$\iint_S [\boldsymbol{J}^* \cdot K(\boldsymbol{J}) - \boldsymbol{J}^* \cdot \frac{1}{2}\hat{n} \times \boldsymbol{J} + \frac{1}{\eta_0^2}\boldsymbol{J}^* \cdot L(\boldsymbol{M})]dS = \iint_S \boldsymbol{J}^* \cdot \boldsymbol{H}^i dS \tag{4}$$

In these equations, $\boldsymbol{E}^i$ and $\boldsymbol{H}^i$ are incident fields, L are K operators involving the free-space Green's function as defined in.

To take advantage of the rotational symmetry of the problem, the fields and the surface currents are expanded in the Fourier modes as :

$$\boldsymbol{E} = \sum_{m=-\infty}^{+\infty} \left[\boldsymbol{E}_{t,m}(\rho, z) - \hat{\phi} E_{\phi,m}(\rho, z) \right] e^{jm\phi} \tag{5}$$

$$\boldsymbol{J} = \sum_{m=-\infty}^{+\infty} \left[\sum_{i=1}^{N_s-1} (a_{m,i}^t \frac{T_i}{\rho}\hat{t} - a_{m,i}^t \frac{T_i}{\rho}\hat{\phi}) \right] e^{jm\phi} \tag{6}$$

$$\boldsymbol{M} = \sum_{m=-\infty}^{+\infty} \left[\sum_{i=1}^{N_s-1} (b_{m,i}^t \frac{T_i}{\rho}\hat{t} - b_{m,i}^t \frac{T_i}{\rho}\hat{\phi}) \right] e^{jm\phi} \tag{7}$$

where N_s is the number of segments along angular cross section of the boundary S, T_i is a standard triangular basis function, the tangential direction $\hat{t}$ is defined by $\hat{t} = \hat{n} \times \hat{\phi}$. The unknown field $\boldsymbol{E}_{t,m}$ and $E_{\phi,m}$ is expanded as:

$$\boldsymbol{E}_{t,0} = \sum_{i=1}^{8} e_{t,i}^e \boldsymbol{N}_i^e \ , \quad E_{\phi,0} = \sum_{i=1}^{8} e_{\phi,i}^e N_i^e \ , \tag{8}$$

for $m = 0$;

$$\boldsymbol{E}_{t,\pm 1} = \mp j\hat{\rho} E_{\phi,\pm 1} + \sum_{i=1}^{8} e_{t,i}^e \rho \boldsymbol{N}_i^e \ , \quad E_{\phi,0} = \sum_{i=1}^{8} e_{\phi,i}^e N_i^e \ , \tag{9}$$

for $m = \pm 1$;

$$\boldsymbol{E}_{t,0} = \sum_{i=1}^{8} e_{t,i}^e \rho \boldsymbol{N}_i^e \ , \quad E_{\phi,0} = \sum_{i=1}^{8} e_{\phi,i}^e N_i^e \ , \tag{10}$$

for $|m| > 1$,

where N_i^e and $\boldsymbol{N}_i^e$ are the second-order hierarchical scalar base functions [9] and vector base functions [10] for triangular element, respectively.

The expansions (5), (6) and (7) are substitued into (1), (3) and (4), and the Rayleigh-Ritz approach is used, where the weight functions are chosen to be equal to the basis function. This process yields a symmetric matrix equation:

$$\begin{pmatrix} Z_m^{FE} & B_m^{EJ} & 0 \\ B_m^{EJ} & G_m^{JJ} & G_m^{JM} \\ 0 & G_m^{MJ} & G_m^{MM} \end{pmatrix} \begin{pmatrix} e_m \\ a_m \\ b_m \end{pmatrix} = \begin{pmatrix} 0 \\ V_m^J \\ V_m^M \end{pmatrix}, \tag{11}$$

Z_m^{FE}, B_m^{EJ} and B_m^{EJ} are sparse finite element matrix, and G_m^{JJ}, G_m^{JM}, G_m^{MJ} and G_m^{MM} are dense moment matrix. The oscillating integrals is evaluated accurately and efficiently to accelerate the generation of the elements of the method of moments' matrix [2].

The above procedure should in principle be carried out for each of the Fourier modes $m = 0, \pm 1, \pm 2, \cdots$. In practice, however, a rule of truncating the infinite Fourier modes for plane wave incidence is $M_{\max} = k_0 \rho_{\max} \sin(\theta) + 6$ [5], where $\rho_{\max}$ is the largest cylindrical radius of the body. Such a rule is valid for $k_0 \rho_{\max} \sin(\theta) > 3$. Furthermore, the solution for each negative modes ($m < 0$) is simply related to that of the corresponding positive modes ($m > 0$). Hence the solutions need to be computed for the nonnegative modes only.

III. Numerical Examples

In this section, numerical results are presented to show the validity and accuracy of the proposed technique. In all examples, the interior FEM mesh length is chosen as about $\lambda/10$, and the boundary mesh length is chosen as about $\lambda/15$, where λ is the free space wavelength.

First，we consider an anisotropic spherical cloak with free space inside. The cloak is characterized in spherical coordinates by a relative permittivity of (12), which is transformed into cylindrical coordinates shown in [11]. The sphere has outer radius $R_2 = 1$ m and inner radius $R_1 = 0.5$, and is characterized by $\varepsilon_R = R_2(r - R_1)^2 / (R_2 - R_1)r^2$ and $\varepsilon_\theta = R_2 / (R_2 - R_1)$. It should be note that at the inner boundary $r = R_1$, the material properties of the cloak behaves an unavoidable singular with $\varepsilon_R = 0$, which lead to theoretically outside the domain of application of the finite-element method. However, the numerical results shows that the cloak can be simulated by the presented method. The interior FEM mesh length is chosen as about $\lambda/15$ and the boundary is set 1λ away from the cloak. Fig. 1 illustrates the real parts of E_y in the xz plane when the plane wave is incident at 15GHz with the angle of incidence $\theta^i = 180^0$ or $\theta^i = 30^0$. From the figure, we observe that the cloaking effect is very clear and the plane wave is almost unaltered outside the cloaking shell, which is nearly the same as the analytical result. Also, the electric field inside the cloaked region is nearly zero with a maximum leakage about 0.3% of the radiating field into the cloaked region, which is more accurate than the result by DDA formalism [12] and FEM with PML [13].

$$\bar{\bar{\mu}}_r = \bar{\bar{\varepsilon}}_r = \varepsilon_R \hat{r}\hat{r} + \varepsilon_\theta \hat{\theta}\hat{\theta} + \varepsilon_\theta \hat{z}\hat{z} \tag{12}$$

$$\begin{aligned} \varepsilon_{\rho\rho} &= \varepsilon_R \sin^2\theta + \varepsilon_\theta \cos^2\theta \\ \varepsilon_{\phi\phi} &= (\varepsilon_R - \varepsilon_\theta)\sin\theta\cos\theta \ , \\ \varepsilon_{zz} &= \varepsilon_R \cos^2\theta + \varepsilon_\theta \sin^2\theta \end{aligned} \tag{13}$$

Then, the presented method is applied to simulate a large 3-D cylindrical gradient-index lens [14], which can transform spherical waves to plane waves. The lens is cylindrically symmetric around the z axis. The centre of the lens was located at the origin of the cylindrical coordinate, the radius (R) and the thickness (H) are 0.8 m and 0.4 m respectively, shown in Fig. 2(a). A 3-D electric dipole directing in the y-direction is placed at the point $(0, 0, -0.6m)$ in the Cartesian coordinates to excite spherical waves. The current dipole moment is $Il = 0.025$ Am, and the working frequency is f = 1.2 GHz. The field of the dipole can be easily expanded to Fourier modes.

The parameter of the lens are described by: $\varepsilon_r = \mu_r = 1.83 - (\sqrt{0.4^2 + \rho^2} - 0.4)/0.46$, which can be realized using metamaterials. The far radiation of the gradient-index lens are shown in Fig. 2(b). The results by 3D CG-FFT method are also given in the figure for comparison. Obviously, good agreement is achieved.

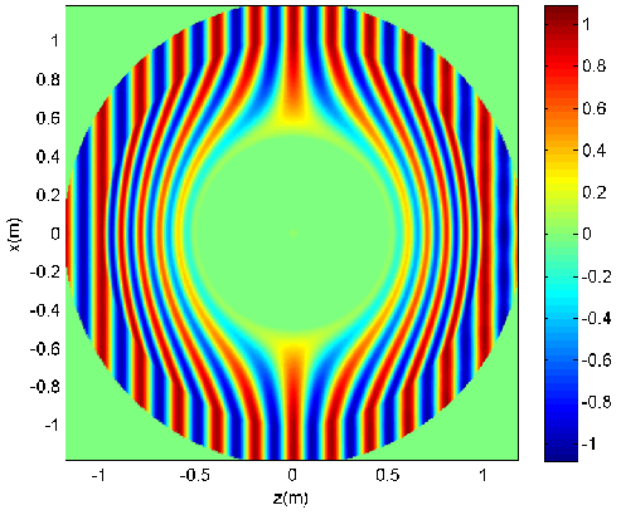

(a) $\theta^i = 180^0$

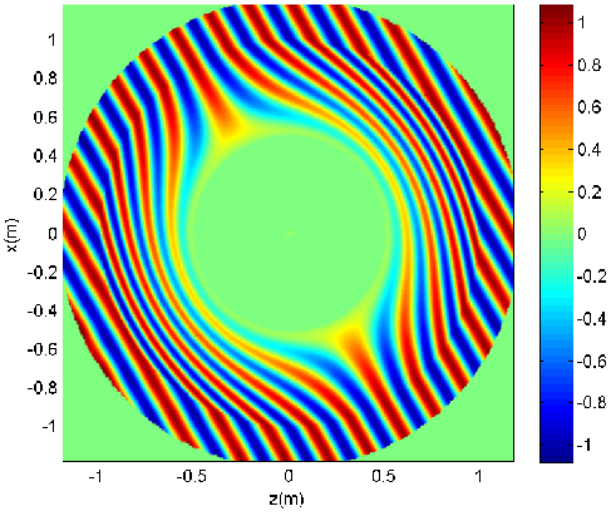

(b) $\theta^i = 30^0$

Figure 1. The real part of the electronic field E_y in the vicinity of the cloaked sphere

IV. CONCLUSIONS

In this paper, we have presented the finite element and boundary integral methods for simulating electromagnetic scattering from complex inhomogeneous bodies of revolution. Numerical examples were presented to demonstrate the accuracy and capability of the method.

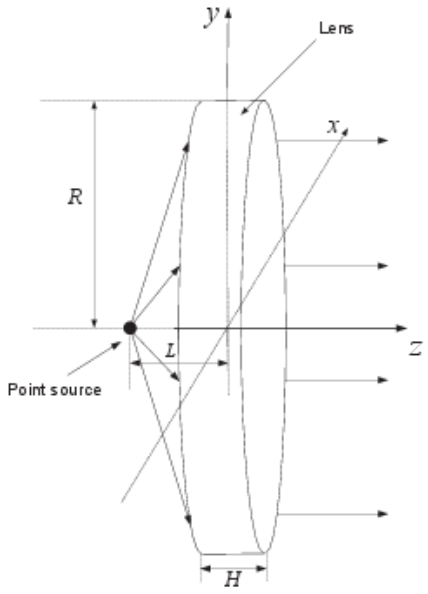

(a)

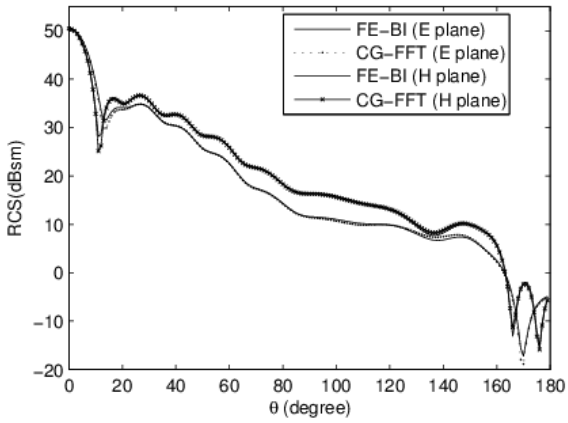

(b)

Figure 2. 3D gradient-index lens and its far field. (a) 3D gradient-index lens excited by point source. (b) far field RCS.

REFERENCES

[1] M. G. Andreasen, "Scattering from bodies of revolution," *IEEE Trans. Antennas Propgat.,* vol. 13, pp. 303-310, Mar. 1965.

[2] W. M. Yu, D. G. Fang and T. J. Cui, "Closed Form Modal Green's Functions for Accelerated Computation of Bodies of Revolution," *IEEE Trans. Antennas Propgat.,* vol. 56, pp. 3452-3461, 2008.

[3] X. Rui, J. Hu and Q. H. Liu.S, "Fast Inhomogeneous Plane Wave Algorithm for Homogeneous Dielectric Body of Revolution," *Microw. Opt. Tech. Lett.,* vol. 52, pp. 1915-1922, 2010.

[4] A. A. Kucharski, "A method of moments solution for electromagnetic scattering by inhomogeneous dielectric bodies of revolution," *IEEE Trans. Antennas Propgat..* vol. 48, pp. 1202-1210, 2000.

[5] A. D. Greenwood and J. M. Jin, "A novel efficient algorithm for scattering from a complex BOR using mixed finite elements and cylindrical PML," *IEEE Trans. Antennas Propgat.,* vol. 47, pp. 620-629, 1999.

[6] D. J. Hoppe and L. W. Epp and J. Lee, "A hybrid symmetric FEM /MOM formulation applied to scattering by inhomogeneous bodies of revolution," *IEEE Trans. Antennas Propgat.,* vol. 42, pp. 798-805, Jun. 1994.

[7] E. A. Dunn and J.K. Byun and E.D. Branch and J.M. Jin, "Numerical simulation of BOR scattering and radiation using a higher order FEM," *IEEE Trans. Antennas Propgat.,* vol. 54, pp. 945-952, Mar. 2006 .

[8] J. M. Jin, "The Finite Element Method in Electromagnetics," New York: Wiley, 1993.
[9] J. P. Webb and S. McFee, "The use of hierarchical triangles in finite-element analysis of microwave and optical devical," *IEEE Trans. Magn.,* vol. 27, pp. 4040-4043, Mar. 1991.
[10] L. S. Andersen and J. L. Volakis, "Development and application of a novel class of hierarchical tangential vector finite elements for electromagnetics," *IEEE Trans. Antennas Propgat.,* vol. 47, pp. 112-120, Jan. 1999.
[11] H. Chen, B. I. Wu, B. Zhang and J. A Kong, "Electromagnetic wave interactions with a metamaterial cloak," *Phys. Rev. Lett.* vol. 99, 063903, 2007.
[12] Y. You, G. W. Kattawar, P. W. Zhai, and P. Yang, "Zero back scatter cloak for aspherical particles using a generalized DDA formalism finite elements for electromagnetics," *Opt. Express.,* vol. 16*,* pp. 2068-2079*,* 2008.
[13] Y. B. Zhai, X. W. Ping, W. X. Jiang, and T. J. Cui, "Finite element analysis of three dimensional axisymmetrical invisibility cloaks and other metamaterial devices," *Commun. Comput. Phys.,* vol. 8*,* pp. 823-834*,* 2010.
[14] H. F. Ma, J. F. Zhang, X. Chen, Q. Cheng and T. J. Cui, "CG-FFT algorithm for three dimensional inhomogeneous and biaxia metamaterials," *Opt. Express.,* vol. 19, pp. 49-64, 2009.